

# Graphical Representation of CP Violation Effects in Neutrinoless Double Beta Decay

K. MATSUDA, N. TAKEDA and T. FUKUYAMA

*Department of Physics, Ritsumeikan University, Kusatsu, Shiga 525-8577, Japan*

H. NISHIURA

*Department of General Education, Junior College of Osaka Institute of Technology, Asahi-ku, Osaka 535-8585, Japan*

(July 19, 2000)

We illustrate the graphical method that gives the constraints on the parameters appearing in the neutrino oscillation experiments and the neutrinoless double beta decay. This method is applicable in three and four generations. Though this method is valid for more general case, we examine explicitly the cases in which the  $CP$  violating factors take  $\pm 1$  or  $\pm i$  in the neutrinoless double beta decay for illustrative clearance. We also discuss some mass matrix models which lead to the above  $CP$  violating factors.

PACS number(s): 14.60.Pq, 11.30.Er, 23.40.Bw

From the recent neutrino oscillation experiments [1] it becomes affirmative that neutrinos have masses. The present and near future experiments enter into the stage of precision test for masses and lepton mixing angles. In a series of papers we have discussed the relations among the parameters which appear in the neutrino oscillation experiments and in the neutrinoless double beta decay  $((\beta\beta)_{0\nu})$  experiments. The most recent experimental upper bound for the averaged mass  $\langle m_\nu \rangle_{ee}$  for Majorana neutrinos from  $(\beta\beta)_{0\nu}$  is given by  $\langle m_\nu \rangle_{ee} < 0.2eV$  [2]. The next generation experiment GENIUS [3] is anticipated to reach a considerably more stringent limit  $\langle m_\nu \rangle_{ee} < 0.01 - 0.001eV$ . In these situations the investigation of the  $CP$  violation effects in the lepton sector has become more and more important. In the previous paper we proposed [4] the graphical method for obtaining the constraints on  $CP$  violation phases from  $(\beta\beta)_{0\nu}$  and neutrino oscillation experiments. This method enables us to grasp the geometrical relations among the parameters of masses, mixing angles,  $CP$  phases etc. and obtain the constraints on them more easily than the analytical calculations [5] [6] [7]. In this letter we apply this method to obtain the constraints on  $\langle m_\nu \rangle_{ee}$  for the given  $CP$

phases. For illustrative purpose we consider the specific values of  $CP$  phases which are partly supported by theoretical models [8]. We also discuss some matrix models which lead to the above  $CP$  phases.

The averaged mass  $\langle m_\nu \rangle_{ee}$  obtained from  $(\beta\beta)_{0\nu}$  is given [9] by the absolute values of averaged complex masses for Majorana neutrinos as

$$\langle m_\nu \rangle_{ee} = |M_{ee}|. \quad (1)$$

Here the averaged complex mass  $M_{ee}$  is defined by

$$M_{ee} \equiv \sum_{j=1}^3 U_{ej}^2 m_j \quad (2)$$

$$\equiv |U_{e1}|^2 m_1 + |U_{e2}|^2 e^{2i\beta} m_2 + |U_{e3}|^2 e^{2i(\rho-\phi)} m_3, \quad (3)$$

after suitable phase convention. The  $CP$  violating effects are invoked in  $\beta$ ,  $\rho$  and  $\phi$  appearing in  $U$ . Here  $U_{aj}$  is the Maki-Nakagawa-Sakata (MNS) left-handed lepton mixing matrix which combines the weak eigenstate neutrino ( $a = e, \mu$  and  $\tau$ ) to the mass eigenstate neutrino with mass  $m_j$  ( $j=1,2$  and  $3$ ). The  $U$  takes the following form in the standard representation [5]:

$$U = \begin{pmatrix} c_1 c_3 & s_1 c_3 e^{i\beta} & s_3 e^{i(\rho-\phi)} \\ (-s_1 c_2 - c_1 s_2 s_3 e^{i\phi}) e^{-i\beta} & c_1 c_2 - s_1 s_2 s_3 e^{i\phi} & s_2 c_3 e^{i(\rho-\beta)} \\ (s_1 s_2 - c_1 c_2 s_3 e^{i\phi}) e^{-i\rho} & (-c_1 s_2 - s_1 c_2 s_3 e^{i\phi}) e^{-i(\rho-\beta)} & c_2 c_3 \end{pmatrix}. \quad (4)$$

Here  $c_j = \cos \theta_j$ ,  $s_j = \sin \theta_j$  ( $\theta_1 = \theta_{12}$ ,  $\theta_2 = \theta_{23}$ ,  $\theta_3 = \theta_{31}$ ). Note that three  $CP$  violating phases,  $\beta$ ,  $\rho$  and  $\phi$  appear in  $U$  for Majorana neutrinos. [10].

Defining the relative  $CP$  violating factors in  $M_{ee}$  by

$$\eta_2 \equiv e^{2i\beta}, \quad \eta_3 \equiv e^{2i(\rho-\phi)} \equiv e^{2i\rho'}, \quad (5)$$

we have

$$M_{ee} = |U_{e1}|^2 m_1 + |U_{e2}|^2 \eta_2 m_2 + |U_{e3}|^2 \eta_3 m_3 \quad (6)$$

Let us review briefly the graphical representations [4] of the complex mass  $M_{ee}$ . We now rewrite the complex mass  $M_{ee}$  as

$$M_{ee} = |U_{e1}|^2 \widetilde{m}_1 + |U_{e2}|^2 \widetilde{m}_2 + |U_{e3}|^2 \widetilde{m}_3 \quad (7)$$

Here we have defined the complex masses  $\widetilde{m}_i (i = 1, 2, 3)$  by

$$\begin{aligned}\widetilde{m}_1 &\equiv m_1, & \widetilde{m}_2 &\equiv \eta_2 m_2 = e^{2i\beta} m_2, \\ \widetilde{m}_3 &\equiv \eta_3 m_3 = e^{2i\rho'} m_3,\end{aligned}\quad (8)$$

The  $M_{ee}$  is the "averaged" complex mass of the masses  $\widetilde{m}_i (i = 1, 2, 3)$  weighted by three mixing elements  $|U_{ej}|^2 (j = 1, 2, 3)$  with the unitarity constraint  $\sum_{j=1}^3 |U_{ej}|^2 = 1$ . Therefore, the position of  $M_{ee}$  in a complex mass plane is within the triangle formed by the three vertices  $\widetilde{m}_i (i = 1, 2, 3)$  if the magnitudes of  $|U_{ej}|^2 (j = 1, 2, 3)$  are unknown (Fig.1). This triangle is referred to as the complex-mass triangle [4]. The three mixing elements  $|U_{ej}|^2 (j = 1, 2, 3)$  indicate the division ratios for the three portions of each side of the triangle which are divided by the parallel lines to the side lines of the triangle passing through the  $M_{ee}$ . (Fig.2). The  $CP$  violating phases  $2\beta$  and  $2\rho'$  represent the rotation angles of  $\widetilde{m}_2$  and  $\widetilde{m}_3$  around the origin, respectively. Since  $\langle m_\nu \rangle_{ee} = |M_{ee}|$ , the present experimental upper bound on  $\langle m_\nu \rangle_{ee}$  (we denote it  $\langle m_\nu \rangle_{max}$ .) indicates the maximum distance of the point  $M_{ee}$  from the origin and forms the circle in the complex plane.

So far we have discussed in the scheme of the three flavour mixings. The sterile neutrino is not ruled out yet [11]. We can easily incorporate the sterile neutrino in our formulation.  $M_{ee}$  is written in this case as

$$\begin{aligned}M_{ee} &= \sum_{j=1}^4 |U_{ej}|^2 \widetilde{m}_j = |U_{e1}|^2 \widetilde{m}_1 + |U_{e2}|^2 \widetilde{m}_2 \\ &\quad + (|U_{e3}|^2 + |U_{e4}|^2) \frac{|U_{e3}|^2 \widetilde{m}_3 + |U_{e4}|^2 \widetilde{m}_4}{|U_{e3}|^2 + |U_{e4}|^2} \\ &\equiv |U_{e1}|^2 \widetilde{m}_1 + |U_{e2}|^2 \widetilde{m}_2 + |U_{e34}|^2 \widetilde{m}_{34}\end{aligned}\quad (9)$$

and Fig.2 is modified as Fig.3.

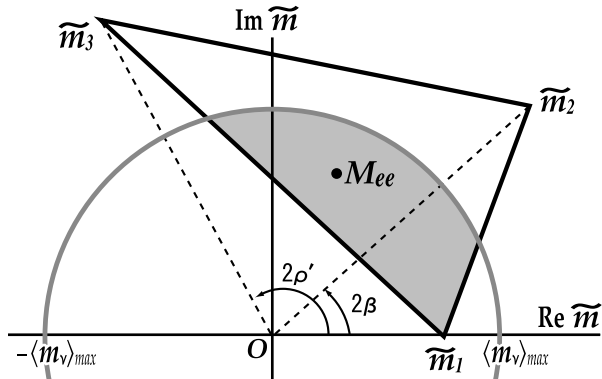


FIG.1 Graphical representations of the complex mass  $M_{ee}$  and  $CP$  violating phases. The position of  $M_{ee}$  is within the triangle formed by the three points  $\widetilde{m}_i (i = 1, 2, 3)$  which are defined in Eq. (8). The allowed position of  $M_{ee}$  is in the intersection (shaded area) of the inside of this triangle and the inside of the circle of radius  $\langle m_\nu \rangle_{max}$  around the origin.

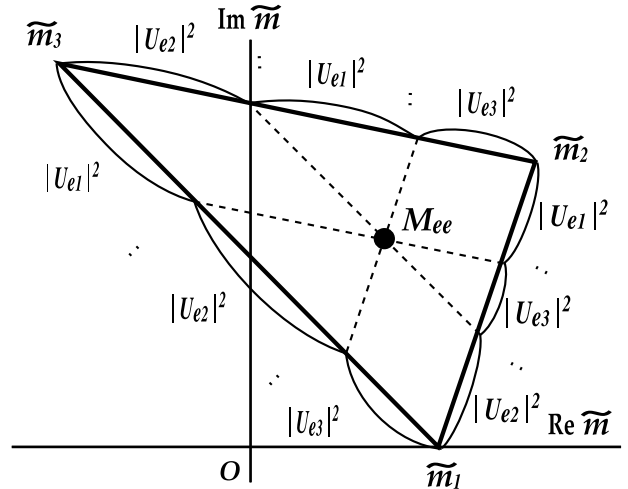


FIG.2 The relations between the position  $M_{ee}$  and  $U_{ei} (i = 1, 2, 3)$  components of MNS mixing matrix.

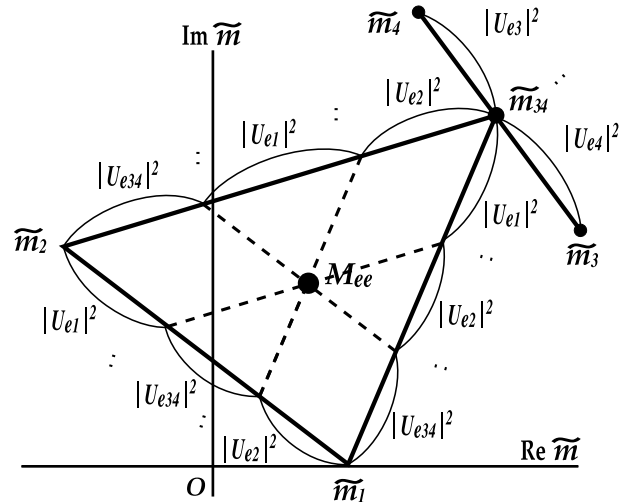


FIG.3 Complex-mass "triangle" for four generations. Complex-mass tetragon formed by the four vertices,  $\widetilde{m}_j (j = 1 - 4)$ , is reduced to "triangle" by (9).

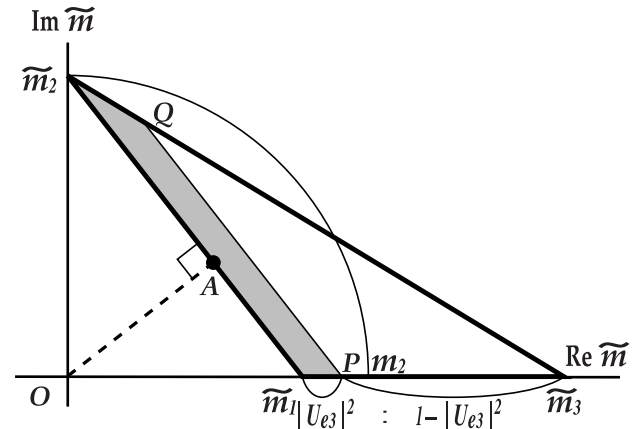


FIG.4 Complex-mass triangle supplemented with  $|U_{e3}|^2 < 0.026$  for  $\eta_2 = i$  and  $\eta_3 = 1$ . The shaded region is allowed. The minimum of  $|M_{ee}|$  is  $\overline{OA}$ . The maximum of  $|M_{ee}|$  changes depending on whether  $|U_{e3}|^2_{max}$  is larger than  $(m_2 - m_1)/(m_3 - m_1)$  or not.

	$\eta_2 = 1$	$\eta_2 = -1$	$\eta_2 = \pm i$
$\eta_3 = 1$	$m_1 \leq \langle m_\nu \rangle_{ee} \leq A_2$	$0 \leq \langle m_\nu \rangle_{ee} \leq \max\left(\frac{m_2}{A_1}\right)$	$B_{12} \leq \langle m_\nu \rangle_{ee} \leq \max\left(\frac{m_2}{A_1}\right)$
$\eta_3 = -1$	$\max\left(\frac{0}{C}\right) \leq \langle m_\nu \rangle_{ee} \leq \max\left(\frac{m_2}{-C}\right)$	$0 \leq \langle m_\nu \rangle_{ee} \leq A_2$	$\max\left(\frac{0}{D_{21}}\right) \leq \langle m_\nu \rangle_{ee} \leq \max\left(\frac{m_2}{E_{23}}\right)$
$\eta_3 = \pm i$	(i) $ U_{e3} _{max}^2 < m_1^2/(m_1^2 + m_3^2)$ , $E_{13} \leq \langle m_\nu \rangle_{ee} \leq \max\left(\frac{m_2}{E_{23}}\right)$ (ii) $ U_{e3} _{max}^2 \geq m_1^2/(m_1^2 + m_3^2)$ , $B_{13} \leq \langle m_\nu \rangle_{ee} \leq \max\left(\frac{m_2}{E_{23}}\right)$	$0 \leq \langle m_\nu \rangle_{ee} \leq \max\left(\frac{m_2}{E_{23}}\right)$	$B_{12} \leq \langle m_\nu \rangle_{ee} \leq A_2$
$\eta_3 = \mp i$	—————	—————	$\max\left(\frac{0}{D_{12}}\right) \leq \langle m_\nu \rangle_{ee} \leq \max\left(\frac{m_2}{E_{23}}\right)$

TABLE I. Given the  $\eta_i = \pm 1$  or  $\pm i$ , the constraints on the averaged mass  $\langle m_\nu \rangle_{ee}$  are given. Notations are as follows.  $|U_{e3}|_{max}^2 = 0.026$ ,  $A_i \equiv m_i + |U_{e3}|_{max}^2(m_3 - m_i)$ ,  $B_{ij} \equiv m_i m_j / \sqrt{m_i^2 + m_j^2}$ ,  $C \equiv m_1 - |U_{e3}|_{max}^2(m_1 + m_3)$ ,  $D_{ij} \equiv m_i(m_j - |U_{e3}|_{max}^2(m_j + m_3)) / \sqrt{m_i^2 + m_j^2}$  and  $E_{ij} \equiv \sqrt{(1 - |U_{e3}|_{max}^2)^2 m_i^2 + |U_{e3}|_{max}^4 m_j^2}$ . The  $\max(a, b)^T$  indicates the larger value between  $a$  and  $b$ . The double signs of  $\eta_2$  and  $\eta_3$  are in the same order.

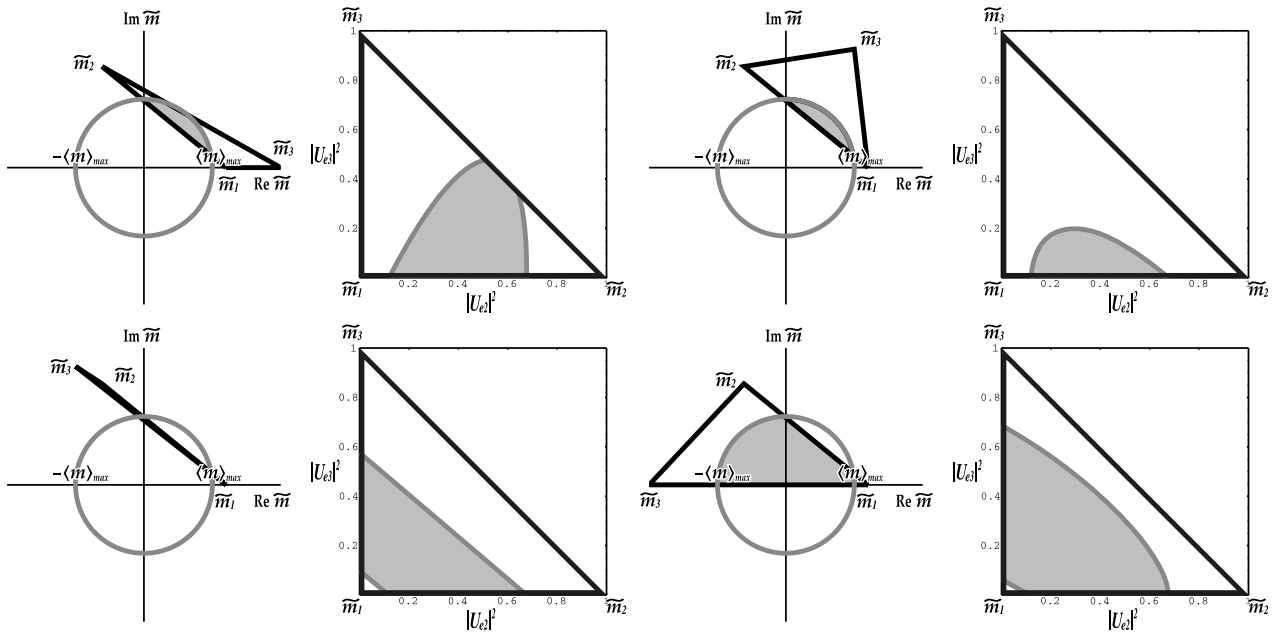


FIG.5 The graph shows the allowed region of  $|U_{e2}|^2$  and  $|U_{e3}|^2$ . The mixing elements  $|U_{ei}|^2$  are expressed as the ratios of the heights from vertices  $m_i$  separated by  $M_{ee}$  (Fig.2). The mass triangle (left diagrams) is deformed to the isosceles right triangle (right diagrams) retaining these ratios. This figure is depicted setting  $m_1 : m_2 : m_3 : \langle m \rangle_{ee} = 6 : 8 : 10 : 5$  and  $2\beta = 5\pi/8$  as an example.  $2\rho'$  is changed every  $\pi/3$ . There is no allowed region in upper-right half, because  $|U_{e2}|^2 + |U_{e3}|^2 = 1 - |U_{e1}|^2 \leq 1$  from unitarity conditions.

We proceed to discuss the main theme to give the constraints on  $\langle m_\nu \rangle_{ee}$ , given  $\eta_i = \pm 1$  or  $\pm i$ . We argue here in the three generations, though the arguments can be extended to the four generation case. We list up the constraints on  $\langle m_\nu \rangle_{ee}$  for the various combinations of given  $CP$  violating factors  $\eta_i$  and explain how our formulation works. (TABLE I)

We demonstrate the graphical method for  $\eta_2 = i$  and  $\eta_3 = 1$  case. In this case Fig.1 becomes Fig.4. Here we impose the constraint on  $U_{e3}$  from the oscilla-

tion experiments of CHOOZ and SuperKamiokande [12],  $|U_{e3}|^2 < 0.026$ . The shaded region is allowed.  $\langle m_\nu \rangle_{ee}$  is the distance from the origin to the shaded region. So the minimum and maximum of  $\langle m_\nu \rangle_{ee}$  is easily estimated from Fig.4. Obviously, the minimum is  $\overline{OA}$ . The maximum value depends on whether the line  $PQ$  crosses the horizontal axis at a point larger than  $m_2$  or not. If  $\overline{OP} > m_2$ , the maximum is  $\overline{OP}$ . If  $\overline{OP} < m_2$ , the maximum becomes  $m_2$ .

Of course, our method is applicable for arbitrary

phases. Using Figs.1 and 2, we can provide the constraints on the mixing elements  $|U_{ei}|$  by changing the complex-mass triangle to the isosceles right triangle (Fig.5).

Next let us discuss a mass matrix model which gives the typical  $CP$  violating phases demonstrated above. In order to see the meaning of  $\eta = \pm 1$  or  $\pm i$  clearly, we first discuss in two generations. We show that the following democratic type of complex mass matrix,

$$\begin{pmatrix} M & M^* \\ M^* & M \end{pmatrix} \quad (10)$$

gives the  $CP$  violating factor  $\eta_2 = i$ . Here the matrix elements  $M^*$  is the complex conjugate of  $M$ . This matrix is diagonalized by a maximal mixing matrix and two mass eigen values remain to be independent free parameters as is shown

$$\begin{pmatrix} \frac{1}{\sqrt{2}} & \frac{1}{\sqrt{2}} \\ -\frac{1}{\sqrt{2}} & \frac{1}{\sqrt{2}} \end{pmatrix} \begin{pmatrix} M & M^* \\ M^* & M \end{pmatrix} \begin{pmatrix} \frac{1}{\sqrt{2}} & -\frac{1}{\sqrt{2}} \\ \frac{1}{\sqrt{2}} & \frac{1}{\sqrt{2}} \end{pmatrix} \\ = \begin{pmatrix} m_1 & 0 \\ 0 & im_2 \end{pmatrix}, \quad (11)$$

where

$$m_1 \equiv 2\text{Re}M, \quad m_2 \equiv 2\text{Im}M. \quad (12)$$

This argument is generalized to the three generations as follows. We consider a model in which the mass matrices for the charged leptons and the Majorana neutrinos,  $M_e$  and  $M_\nu$ , are given by

$$M_e = \text{diag}(m_e, m_\mu, m_\tau), \quad (13)$$

$$M_\nu = \begin{pmatrix} c_3 & 0 & s_3 \\ -s_2s_3 & -c_2 & s_2c_3 \\ -c_2s_3 & s_2 & c_2c_3 \end{pmatrix} \\ \times \begin{pmatrix} M & M^* & 0 \\ M^* & M & 0 \\ 0 & 0 & m_3 \end{pmatrix} \begin{pmatrix} c_3 & 0 & s_3 \\ -s_2s_3 & -c_2 & s_2c_3 \\ -c_2s_3 & s_2 & c_2c_3 \end{pmatrix}^T. \quad (14)$$

Then, the mass matrix  $M_\nu$  is diagonalized by an orthogonal matrix  $O_\nu$  with a pure imaginary eigenvalue for the second generation neutrino as

$$O_\nu^T M_\nu O_\nu = \begin{pmatrix} m_1 & & \\ & im_2 & \\ & & m_3 \end{pmatrix}, \quad (15)$$

where

$$O_\nu = \begin{pmatrix} c_1c_3 & s_1c_3 & s_3 \\ -s_1c_2 - c_1s_2s_3 & c_1c_2 - s_1s_2s_3 & s_2c_3 \\ s_1s_2 - c_1c_2s_3 & -c_1s_2 - s_1c_2s_3 & c_2c_3 \end{pmatrix}. \quad (16)$$

with the maximal mixing for  $\theta_1$ . Namely the assumption Eq.(14) leads to a pure imaginary eigenvalue  $im_2$  and a

maximal mixing  $c_1 = s_1 = \pi/4$ . Here  $m_1$  and  $m_2$  are defined in (12). The mass matrix is finally diagonalized with real diagonalized masses as

$$U_\nu^T M_\nu U_\nu = \begin{pmatrix} m_1 & & \\ & m_2 & \\ & & m_3 \end{pmatrix}, \quad (17)$$

where

$$U_\nu = O_\nu \begin{pmatrix} 1 & & \\ & e^{i\frac{\pi}{4}} & \\ & & 1 \end{pmatrix}. \quad (18)$$

This mass matrix model corresponds to the case with  $\eta_2 = i$  and  $\eta_3 = 1$  discussed before.

The work of K.M. is supported by the JSPS Research Fellowship, No.10421.

- 
- [1] T.Kajita, talk presented at Neutrino '98 (Takayama, Japan, June 1998).
  - [2] L. Baudis et al., Phys. Rev Lett. **83** 41 (1999).
  - [3] J. Hellmig, H.V. Klapdor-Kleingrothaus, Z.Phys. **A 359** 361 (1997); H.V. Klapdor-Kleingrothaus, M. Hirsch, Z.Phys. **A 359** 382 (1997); L. Baudis et al., Phys. Rep. **307** 301 (1998).
  - [4] K. Matsuda, N. Takeda, T. Fukuyama, and H. Nishiura, to appear in Phys. Rev. **D** (hep-ph/0003055).
  - [5] T. Fukuyama, K. Matsuda, and H. Nishiura, Phys. Rev. **D57** 5844 (1998).
  - [6] T. Fukuyama, K. Matsuda, and H. Nishiura, Mod. Phys. Lett. **A13** 2279 (1998).
  - [7] H. Nishiura, K. Matsuda, and T. Fukuyama, Mod. Phys. Lett. **A14** 433 (1999).
  - [8] K. Fukuura, T. Miura, E. Takasugi and M. Yoshimura, Phys. Rev. **D61** 073002 (2000).
  - [9] M. Doi, T. Kotani, H. Nishiura, K. Okuda and E. Takasugi, Phys. Lett. **102B** 323 (1981); M. Doi, T. Kotani and E. Takasugi, Prog. Theor. Phys. Suppl. **83** 1 (1985); W.C. Haxton and G.J. Stophenson Jr., Prog. Part. Nucl. Phys. **12** 409 (1984).
  - [10] S.M. Bilenky, J. Hosek and S.T. Petcov, Phys. Lett. **94B** 495 (1980); J. Schechter and J.W.F. Valle, Phys. Rev. **D22** 2227 (1980); M. Doi, T. Kotani, H. Nishiura, K. Okuda and E. Takasugi, Phys. Lett. **102B** 323 (1981); A. Barroso and J. Maalampi, Phys. Lett. **132B** 355 (1983).
  - [11] E. Lisi, talk presented at Neutrino 2000 (Sudbury, Canada, June 16-21 2000).
  - [12] M. Apollonio et al., Phys. Lett. **B466** 415 (1999) and Phys. Lett. **B338**, 383 (1998).